TELKOMNIKA Telecommunication, Computing, Electronics and Control
Vol. 22, No. 5, October 2024, pp. 1053∼1060
ISSN: 1693-6930, DOI: 10.12928/TELKOMNIKA.v22i5.26064

Design of high gain and wideband circular patch antenna based on DGS for 28 GHz 5G applications

Md. Sohel Rana[1,2], Md. Nahid Hasan[1], Mohammad Faisal[2], Md. Emran Khan[1]
[1]Department of Electrical and Electronic Engineering, Daffodil International University, Dhaka, Bangladesh
[2]Department of Electrical and Electronic Engineering, Bangladesh University of Engineering and Technology (BUET), Dhaka, Bangladesh

Article Info

Article history:

Received Feb 8, 2024
Revised Mar 13, 2024
Accepted Mar 29, 2024

Keywords:

Circular patch antenna
Defected ground structures
Enhanced bandwidth
Enhanced gain
Improved reflection coefficient

ABSTRACT

In this study, a single band 28 GHz antenna with defected ground structure (DGS) has been proposed. The integration of a DGS is explored to exploit ground plane defects for achieving wideband operation. Through systematic design and optimization, our approach achieves remarkable bandwidth enhancement, expanding from 0.75 GHz to 5.78 GHz, covering frequencies from 26.43 GHz to 32.21 GHz, resulting in an impressive impedance bandwidth of 20.5%. Notably, the proposed methodology significantly improves the reflection coefficient, reducing it from -16 dB to -57 dB. Furthermore, the antenna demonstrates a gain of 5.123 dBi and an enhanced voltage standing wave ratio (VSWR) of 1.0056348. Comparative analysis against existing works underscores the superior performance of our antenna design, affirming its potential for various applications. This work presents a novel DGS featuring a circular microstrip patch antenna (MPA) with dimensions of 8×8×0.5 m³, utilizing Rogers RT5880LZ substrate (ε=2) with a thickness of 0.5 mm.

Corresponding Author:

Md. Sohel Rana
Department of Electrical and Electronic Engineering, Daffodil International University
Daffodil Smart City (DSC), Birulia, Savar, Dhaka-1216, Bangladesh
Email: sohel.eee@diu.edu.bd

1. INTRODUCTION

The mmWave spectrum refers to a range of radio frequencies typically between 30-300 GHz is a key component of 5G cellular networks which is anticipated to be dominant because of its high rate of data transmission to fulfill the needs of the proliferation of 5G applications [1]. The frequency bands of interest for the 5G are 28, 38, 60, and 73 GHz [2]. In contemporary times, the swift evolution of microwave technology has led to an increasing need for expanded bandwidth [3]. Unlike traditional microwave antennas, microstrip patch antennas (MPAs) encounter limitations including reduced gain, significant ohmic loss within the array, and primarily radiating energy into half space. Their practical application is hindered by their limited bandwidth [4]–[6]. Microstrip antennas' limited bandwidth necessitates wideband antenna selection for energy harvesting, capturing a broader spectrum of RF energy for more effective DC power conversion [7]. Traditional MPAs, with a bandwidth typically between 1% to 2%, face limitations due to their resonant nature and thin profile. Research efforts are directed towards broadening their frequency coverage to enhance suitability for diverse applications [8]. The primary challenge in designing MPAs lies in achieving both wide bandwidth and increased gain concurrently [9]. Over the preceding years, various approaches have been suggested to augment the bandwidth of MPAs, including strategies like elevating the substrate thickness [10], lowering the dielectric constant of the substrate [11], employing parasitic patches in both single layer and multi layer configurations [12], utilizing electromagnetic band gap structures [13], employing a backed edge-fed cavity [14]. Recently defected ground structures (DGS) are introduced in antenna design. DGS involves etching patterns into the ground plane to suppress unwanted frequencies and enhance bandwidth [15]. Integrating DGS into MPAs offers a strategy for multi-band support and operation across various frequencies within a single device. Different DGS types provide advantages like reducing antenna size and improving bandwidth [16]. Farahat and Hussein [17], a compact dual-band antenna with a modified ground plane exhibits operational bandwidths of approximately 1.23 GHz at 28 GHz and 1.06 GHz at 38 GHz. Despite the adjustment in the ground plane, notable enhancements in bandwidth are not observed. Surendran *et al.* [18] utilizing a 3×3 array of radiating patches and a slotted ground plane, a Franklin array element operates in two separate frequency bands: 21.5–24.3 GHz and 33.9–36 GHz. The antennas offer wide operational bandwidth, high gain, and compact size advantages, yet their complex structures pose a hindrance. Khan *et al.* [19], the antenna setup features a defected circular shape radiator with a modified ground plane, operating from 23 to 28 GHz with a maximum gain of 5.85 dB. However, despite its performance, the antenna is relatively large. In contrast, an arc-shaped millimeter-wave antenna offers a bandwidth of 4.41 GHz and a gain of 4.49 dBi [20]. Przesmycki *et al.* [21] the problem with this design is lower gain and poor return loss. Another antenna, with a bandwidth of 5.57 GHz and a gain of 5.09 dBi, was introduced but lacks compactness and failed to achieve satisfactory return loss. Additionally, a 28 GHz resonating antenna incorporating a DGS has been developed as referenced [22]. This antenna boasts a bandwidth of 2.9 GHz and achieves a single element gain of 3.45 dBi. In addressing the constraints observed in prior designs, this paper introduces a compact antenna designed for operation within the mm-wave 5G frequency spectrum. Our proposed DGS techniques boost antenna bandwidth while maintaining a decent gain without adding extra complexity or without increasing its size.

2. DESIGN AND ANALYSIS

Initially, the design of a traditional circular microstrip patch antenna is executed using CST studio software. Subsequently, the software facilitates the simulation of antenna design to gauge its real-world performance. In the process of antenna design, it is presupposed that the substrate's dielectric constant (ε), the resonant frequency (f in GHz), and the substrate height (h in mm) are predetermined. circular patch's radius is determined by [23]:

$$r = \frac{F}{[1 + \frac{2h}{\pi F \epsilon}(ln\frac{\pi F}{2h} + 1.7726)]^{\frac{1}{2}}} \tag{1}$$

$$F = \frac{8.791 \times 10^9}{f\sqrt{\epsilon}} \tag{2}$$

The equations presented earlier have led to the antenna dimensions outlined in Table 1. The design of the antenna is depicted in Figures 1(a)-1(c) based on these calculations. These data will be utilized for optimizing the antenna, focusing on enhancing bandwidth and reducing its overall size. In initial design substrate length (Sy) , substrate width (Sx) , ground length (Gy), and ground width (Gx) are equal.

Table 1. Dimensions of the conventional antenna design

Antenna component	Symbol	Dimensions (mm)
Antenna radius	r	2.3
Substrate length	Sy	8
Substrate height	h	0.5
Ground depth	Gd	0.035
Feed line length	Fy	3.8
Feed line width	Fx	1.6453
Inset length	Iy	2.1
Inset width	Ix	0.25

In the initial phases of antenna design, precision was paramount in crafting a circular patch antenna using (1) and (2) with cst along with a judiciously incorporated 50 Ω power port, ensured efficient energy transfer. Figures 1(a)-1(c) visually articulates the preliminary antenna, which resonated at 27.2 GHz, exhibiting a noteworthy 0.75 GHz bandwidth and 6.71 dBi gain. To enhance the bandwidth and improve the return loss, a highly effective method involves introducing a ground defect, which has proven to work remarkably well. Following this modification, the antenna exhibited remarkable attributes, functioning as a high-bandwidth antenna with improved return loss and enhanced impedance matching. The primary approach involves strategically cutting the ground to reduce its length and width relative to substrate dimensions, denoted as Ax and illustrated in Figure 1(d). Figure 1(e) shows the lateral view of the modified antenna with DGS, highlighting the differences in length and width between the ground plane and substrate. This ground-cutting method resulted in a significant enhancement of bandwidth, increasing from 0.75 GHz to an impressive 5.78 GHz. The antenna resonated at 28.15 GHz, accompanied by a substantially improved reflection coefficient of -43 dB, compared to the previous -17 dBi. This denotes a noteworthy advancement in antenna performance. Further refinement was achieved by introducing an additional ground defect, as depicted in Figure 1(f), involving the removal of a thin circular ring with thickness ’a’. This refinement maintained the resonant frequency at 28 GHz while achieving a more improved reflection coefficient of -57 dB, without compromising the increased bandwidth. These findings underscore the effectiveness of ground-cutting methods in significantly enhancing antenna performance showed in Figure 2(a). Reducing the length and ground dimensions of the preliminary antenna by Ax, while maintaining other dimensions constant, has yielded a significant impact. This modification has resulted in a wide bandwidth with an improved reflection coefficient, as depicted in Figure 2(b). The graph highlights the variations in reflection coefficient and bandwidth corresponding to different values of Ax.

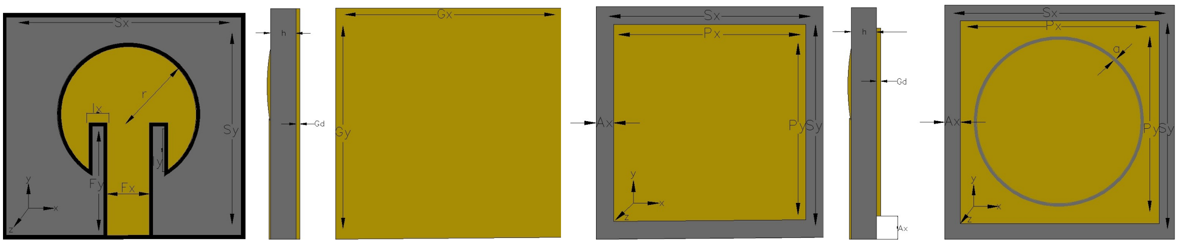

(a) (b) (c) (d) (e) (f)

Figure 1. Conventional circular patch antenna design: (a) front View, (b) side view, (c) back view. Proposed antenna with DGS of: (d) back view with first step (e) side view, and (f) back view with second step of DGS

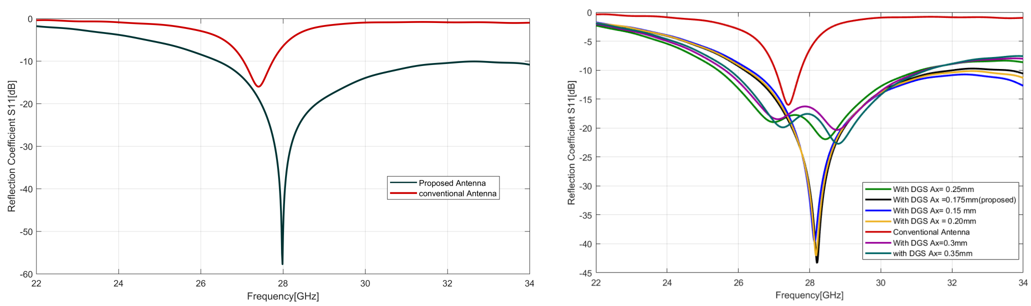

(a) (b)

Figure 2. Comparison of antenna performance between conventional and proposed antenna; (a) bandwidth and reflection coefficient concerning ‘a’ and (b) bandwidth and reflection coefficient concerning Ax

3. PARAMETRIC ANALYSIS

3.1. Effect of reducing ground length and width by (2Ax)

Simulation results reveal a consistent shift in reflection coefficients to a distinct frequency range with each alteration of Ax, consistently hovering around 28 GHz bandwidth. Table 2 enumerates the values obtained from a series of simulations. Notably, the proposed antenna dimensions, specifically with Ax set at 0.175 mm, demonstrate the desired resonant frequency and a notably broader bandwidth. The antenna exhibits a minimal S11 level of -43 dB at 28.2 GHz, accompanied by a bandwidth spanning from 26.43 GHz to 32.21 GHz.

Table 2. Antenna simulation results concerning Ax

Ax (mm)	Bandwidth (GHz)	Reflection coefficient (dB)	Reduced length and width (2Ax)	Resonant frequency (GHz)
0.25	4.8	-23	0.5	28.3
0.175 (proposed)	5.78	-43	0.35	28.2
0.15	5	-39	0.30	28.15
0.20	5.6	-42	0.40	28.2
0.3	5.2	-23	0.6	28.8
0.35	5.3	-23	0.7	28.5

3.2. Effect of trimming a thin circular ring with thickness ‘a’ on the reduced ground dimensions

Through previous simulations, advancements have been achieved in enhancing bandwidth and minimizing return loss by strategically reducing the dimensions of both length and width in the ground plane. A novel technique has been introduced, as depicted in Figure 1(f), involving the removal of an extremely thin circular ring with thickness ‘a’ from the ground while maintaining the constancy of the ground defect Ax. This innovative approach involves the precise trimming of a circular shape with a thickness (a) of 0.005 mm. Remarkably, this adjustment has proven instrumental in attaining an exact resonance frequency at 28 GHz. The efficacy of this method is clearly illustrated in Figure 3(a) and summarized in Table 3, showcasing significant improvements in return loss results for different values of ‘a’ while maintaining a constant value of ’Ax’. The proposed antenna exhibits a remarkable reduction in return loss, registering at S11=-57dB, while resonating precisely at the targeted frequency of 28 GHz showed. Furthermore, this optimization has widened the bandwidth, now spanning from 26.43 GHz to 32.216 GHz. Further experiments were conducted to analyze the effect of varying values of Ax while maintaining a constant thickness ‘a’. The results are illustrated in Figure 3(b) and the corresponding parametric values are detailed in Table 4. These outcomes underscore the success of the introduced circular trimming technique in refining antenna performance and achieving optimal resonance characteristics.

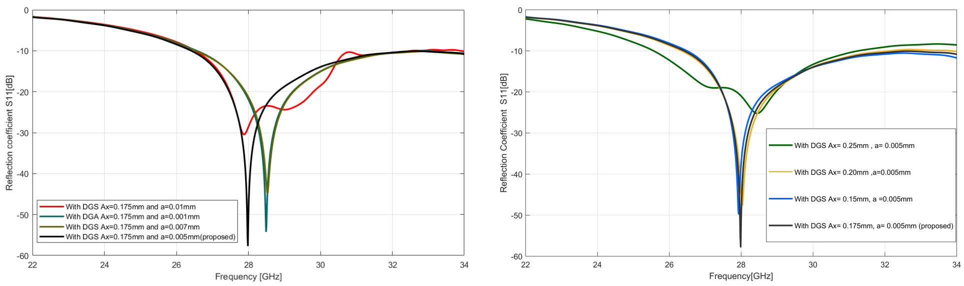

(a) (b)

Figure 3. Comparison of antenna performance concerning the combination of different shapes of DGS; (a) bandwidth and reflection coefficient concerning DGS ‘a’ and (b) bandwidth and reflection coefficient concerning DGS ‘a’ and ‘Ax’

Table 3. Antenna simulation results concerning ‘a’ with constant ‘Ax’

Ax (mm)	a (mm)	Reflection coefficient(dB)	Resonant frequency (GHz)
0.175	0.01	-30	27.9
0.175	0.001	-54	28.5
0.175	0.005 (proposed)	-57	28
0.175	0.007	-44	28.55

Table 4. Antenna simulation results concerning ‘a’

Ax (mm)	a (mm)	Reflection coefficient (dB)	Reduced length and width (2Ax)	Resonant frequency (GHz)
0.25	0.005	-24	0.5	28.3
0.175 (proposed)	0.005	-57	0.35	28
0.15	0.005	-49	0.30	28
0.20	0.005	-47	0.40	28

4. RESULTS AND DISCUSSION

4.1. Voltage standing wave ratio

For a patch antenna, it is essential that the voltage standing wave ratio (VSWR) remains below 2 throughout the entire frequency range. In this case spanning from 26.43 GHz to 32.21 GHz. Figure 4(a) illustrates the relationship between the VSWR, examining the graph, it is evident that throughout the entire frequency range spanning from 26.43 GHz to 32.21 GHz the value of VSWR is less then 2. At the resonance frequency of 28.00 GHz, the VSWR value is measured at 1.005634. Equation of finding VSWR and return loss [24] where, Γ is reflection coefficient:

$$\Gamma = \frac{VSWR - 1}{VSWR + 1} \tag{3}$$

$$ReturnLoss = -20log_{10}\Gamma \tag{4}$$

4.2. Surface current

The surface current distribution analysis at 28 GHz reveals varying maximum current densities along different parts of the circular patch for the designed antenna Figures 4(b) and 4(c). In contrast, the conventional antenna 4(c) primarily concentrates its maximum current strength in the lower middle of the 28 GHz circular patch. Additionally, Figure 4(b) showcases the current distribution of an antenna with a DGS, indicating heightened current concentration in the lower section of the antenna ground, specifically within a segment of the DGS.

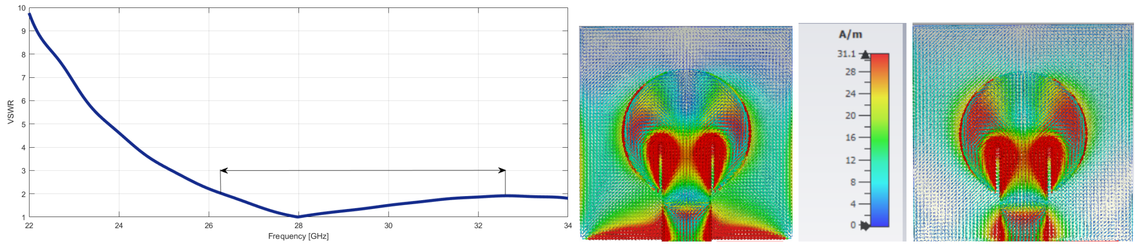

(a) (b) (c)

Figure 4. VSWR and surface currents; (a) the graph depicting the VSWR concerning frequency corresponds to the proposed antenna's operation, (b) proposed antenna's current distribution at 28 GHz, and (c) conventional antennas current distribution at 28 GHz

4.3. Antenna gain and efficiency

In a transmitting antenna, the gain characterizes the efficiency with which the antenna transforms input power into directed radio waves. Conversely, in a receiving antenna, the gain denotes the efficiency with which the antenna converts incoming radio waves from a specific direction into electrical power. In cases where no specific direction is indicated, gain is commonly interpreted as the maximum value of the gain, representing the gain in the direction of the antenna's primary lobe [25]. The suggested antenna exhibits a gain of 5.123 dBi at the resonance frequency of 28.00 GHz, a notably elevated value within the realm of compact microstrip antennas. The graphical representation of antenna gain across different frequencies is illustrated in Figure 5(a). The efficiency of the proposed antenna depicted in Figure 5(b).

4.4. Radiation characteristics

The radiation characteristics illustrate how an antenna emits energy in different directions. This involves depicting a standardized pattern of the electric field or the proportional distribution of surface power density [26]. The desired antenna is expected to demonstrate bidirectional radiation patterns in both the E-plane and H-plane, attributed to the influence of the incorporated DGS. In Figures 6(a) and 6(b), the radiation characteristics of the antenna with a DGS are presented. The findings reveal that the antenna attains a maximum gain of 5.123 dBi, observed in the direction of 12°. Likewise, the three-dimensional radiation pattern incorporating DGS is illustrated in the Figure 6(b). Figures 6(c) and 6(d) depicts the radiation characteristics in the E-plane and H-plane of the conventional antenna without any DGS. The results indicate that the antenna achieves its maximum gain of 6.71 dBi at an azimuthal direction of 6°. Similarly, the three-dimensional radiation pattern without (DGS) is illustrated in the Figure 6(d).

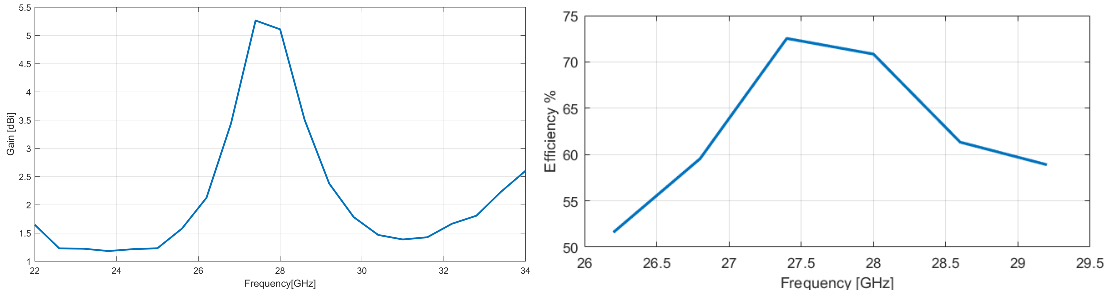

(a) (b)

Figure 5. The graph depicting the antenna gain and efficiency concerning frequency for the proposed antenna; (a) gain and (b) efficiency

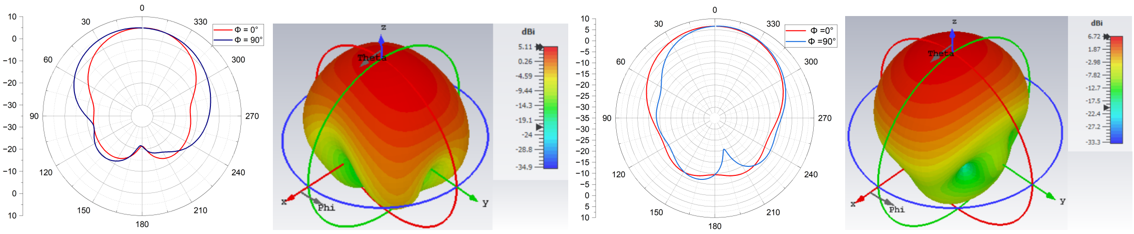

(a) (b) (c) (d)

Figure 6. Radiation patterns for the proposed antenna with DGS and without DGS operating at 28 GHz; (a) E-plan and H-plan without DGS, (b) 3D radiation pattern without DGS, (c) E-plan and H-plan with DGS, and (d) 3D radiation pattern without DGS

4.5. Comparative analysis

The new antenna was compared with recent designs, as shown in Table 5. It is more compact, has reduced height, a wide bandwidth, high gain, and a simple structure. Which making it a strong candidate for 28 GHz 5G applications.

Table 5. Analyze and compare the proposed antenna with those documented in existing literature

References	Dimensions m^3	Resonating frequency (GHz)	Bandwidth (GHz)	Peak gain (dBi)	Reflection coefficient (dB)	Efficiency (%)
[20]	5×3×1.6	28	4.41	4.49	-27	89
[21]	6.2×8.4×1.57	28	5.57	5.06	-23	-
[19]	30×30×0.508	28	5	5.8	-30	80
[27]	1.2×1.2×0.018	28	6.4	5.6	-33	87
[26]	7.43×3.8×0.79	28	2.1	7.41	-30	-
[28]	5.16×3.44×0.55	28	1.95	6.14	-27	-
[29]	10×10×1.575	28	4	7.1	-28	-
[22]	18.85×24×0.254	28	2.9	3.45	-35	88
Proposed	8×8×0.5	28	5.78	5.123	-57	70

5. CONCLUSION

This study introduces a novel design methodology for a circular patch antenna (MPA) integrated with a DGS. By leveraging ground plane defects, our approach achieves significant enhancements in bandwidth, impedance characteristics, reflection coefficient, gain, and VSWR. Through systematic optimization, the antenna's operational bandwidth expands impressively from 0.75 GHz to 5.78 GHz, covering frequencies from 26.43 GHz to 32.21 GHz, with an impedance bandwidth of 20.5%. Notably, the reflection coefficient is improved from -16 dB to -57 dB, demonstrating the effectiveness of the proposed methodology. Comparative analysis against existing works further confirms the superior performance of our antenna design. These results underscore the potential of our approach for various applications in wideband communication systems.

ACKNOWLEDGEMENT

Funded by Divison of Research, Daffodil International University, Bangladesh.

REFERENCES

[1] P. A. Dzagbletey and Y.-B. Jung, "Stacked microstrip linear array for millimeter-wave 5g baseband communication," *IEEE Antennas and Wireless Propagation Letters*,vol. 17, no. 5, pp. 780-783, May 2018, doi: 10.1109/LAWP.2018.2816258.

[2] G. Ancans, V. Bobrovs, A. Ancans, and D. Kalibatiene, "Spectrum considerations for 5g mobile communication systems," *Procedia Computer Science*, vol. 104, pp. 509–516, 2017, doi: 10.1016/j.procs.2017.01.166.

[3] S. Haykin, "Cognitive radio: brain-empowered wireless communications," *IEEE journal on selected areas in communications*, vol. 6, no. 1, 2019, doi: 10.1186/svol. 23, no. 2, pp. 201–220, 2005, doi: 10.1109/JSAC.2004.839380.

[4] L. Tao *et al*., "Bandwidth enhancement of microstrip patch antenna using complementary rhombus resonator," *Wireless Communications and Mobile Computing*, vol. 2018, 2018, doi:10.1155/2018/6352181.0.1109/ACCESS.2019.2895334.

[5] M. S. Rana and M. M. R. Smieee, "Design and analysis of microstrip patch antenna for 5g wireless communication systems," *Bulletin of Electrical Engineering and Informatics*, vol. 11, no. 6, pp. 3329–3337, 2022, doi: 10.11591/eei.v11i6.3955.

[6] M. A. Haque, M. Zakariya, L. C. Paul, D. Nath, P. Biswas, and R. Azim, "Analysis of slotted e-shaped microstrip patch antenna for ku band applications," *2021 IEEE 15th Malaysia International Conference on Communication (MICC)*, Malaysia, 2021, pp. 98-101, doi: 10.1109/MICC53484.2021.9642100.

[7] A. Rajawat, K. M. Agrawal, and P. Singhal, "Design, implementation and analysis of wide-band antenna with novel dgs for rf energy harvesting," *Materials Today: Proceedings*, Mar. 2023, doi: 10.1016/j.matpr.2023.03.456.

[8] S. A. R. Parizi, "Bandwidth enhancement techniques," *Microstrip Antennas: Trends in Research on*, vol. 1, 2017.

[9] J. Tarade and U. P. Khot, "Challenges in optimizing the microstrip patch antenna for endoscopy application," *2023 11th International Conference on Emerging Trends in Engineering & Technology - Signal and Information Processing (ICETET - SIP)*, Nagpur, India, 2023, pp. 1-7, doi: 10.1109/ICETET-SIP58143.2023.10151510.

[10] M. Kara, "The resonant frequency of rectangular microstrip antenna elements with various substrate thicknesses," *Microwave and Optical Technology Letters*, vol. 11, no. 2, pp. 55–59, 1996, doi:10.1002/(SICI)1098.

[11] M. R. Hasan and A. Al Suman, "Substrate height and dielectric constant dependent performance analysis of circular microstrip patch array antennas for broadband wireless access," *American Academic & Scholarly Research Journal*, vol. 4, no. 5, 2012.

[12] A. Katyal and A. Basu, "Compact and broadband stacked microstrip patch antenna for target scanning applications," *IEEE Antennas and Wireless Propagation Letters*, vol. 16, pp. 381–384, 2016, doi:10.1109/LAWP.2016.2578723.

[13] L. Kurra, M. P. Abegaonkar, A. Basu, and S. K. Koul, "Switchable and tunable notch in ultra-wideband filter using electromagnetic bandgap structure," *IEEE Microwave and Wireless Components Letters*, vol. 24, no. 12, pp. 839–841, 2014, doi:10.1109/LMWC.2014.2363020.

[14] K. Fan, Z.-C. Hao, and Q. Yuan, "A low-profile wideband substrate-integrated waveguide cavity-backed e-shaped patch antenna for the q-linkpan applications," *IEEE Transactions on Antennas and Propagation*, vol. 65, no. 11, pp. 5667–5676, 2017, doi: 10.1109/TAP.2017.2748181.

[15] M. K. Khandelwal, B. K. Kanaujia, and S. Kumar "Defected ground structure: fundamentals, analysis, and applications in modern wireless trends," *International Journal of Antennas and Propagation*, vol. 2017, no. 1, 2017, doi: 10.1155/2017/2018527.

[16] M. H. Ali, N. H. Sherif, and G. S. Abd-almuhsen, "Bandwidth enhancement of a microstrip patch antenna using inverted-f shaped defected ground structure," *American Scientific Research Journal for Engineering, Technology, and Sciences (ASRJETS)*, vol. 54, no. 1, pp. 20–29, 2019, doi: 10.1109/TITS.2019.2924883.

[17] A. E. Farahat and K. F. Hussein, "Dual-band (28/38 ghz) wideband mimo antenna for 5g mobile applications," *IEEE Access*, vol. 10, pp. 32213-32223, 2022, doi: 10.1109/ACCESS.2022.3160724.

[18] A. Surendran, T. Ali, O. P. Kumar, P. Kumar, and J. Anguera, "A dual-band modified franklin mm-wave antenna for 5g wireless applications," *Applied Sciences*, vol. 11, no. 2, p. 693, 2021, doi: 10.3390/app11020693.

[19] Z. Khan, M. H. Memon, S. U. Rahman, M. Sajjad, F. Lin, and L. Sun, "A single-fed multiband antenna for wlan and 5g applications," *Sensors*, vol. 20, no. 21, p. 6332, 2020, doi:10.3390/s20216332.

[20] P. Kumar *et al*., "An ultra-compact 28 ghz arc-shaped millimeter- wave antenna for 5g application," *Micromachines*, vol. 14, no. 1, p. 5, 2022, doi:10.3390/mi14010005.

[21] R. Przesmycki, M. Bugaj, and L. Nowosielski, "Broadband microstrip antenna for 5g wireless systems operating at 28 ghz," *Electronics*, vol. 10, no. 1, p. 1, 2020, doi:10.3390/electronics10010001.

[22] S. Khan *et al*., "A compact 28 ghz millimeter wave antenna for future wireless communication," *Computers, Materials & Continua*, vol. 72, no. 1, 2022, doi:10.32604/cmc.2022.023397.

[23] M. Singh, A. Basu, and S. Koul, "Circular patch antenna with quarter wave transformer feed for wireless communication," *2006 annual IEEE India conference*, 2006, pp. 1–5, doi: 10.1109/INDCON.2006.302847.

[24] A. Elrashidi, K. M. Elleithy, and H. Bajwa, "Input impedance, vswr and return loss of a conformal microstrip printed antenna for tm01 mode using two different substrates," *International Journal of Networks and Communications*, vol. 2, no. 2, pp. 13–19, 2012, doi: 110.5923/j.ijnc.20120202.03.

[25] W. L. Stutzman, "Estimating directivity and gain of antennas," *IEEE Antennas and Propagation Magazine*, vol. 40, no. 4, pp. 7–11, 1998, doi: 10.1109/74.730532.

[26] J.-S. Park, J.-B. Ko, H.-K. Kwon, B.-S. Kang, B. Park, and D. Kim, "A tilted combined beam antenna for 5g communications using a 28-ghz band," *IEEE Antennas and Wireless Propagation Letters*, vol. 15, pp. 1685–1688, 2016, doi: 10.1109/LAWP.2016.2523514.

[27] W. A. Awan, S. I. Naqvi, A. H. Naqvi, S. M. Abbas, A. Zaidi, and N. Hussain, "Design and characterization of wideband printed antenna based on dgs for 28 ghz 5g applications," *Journal of Electromagnetic Engineering & Science*,, vol. 21, no. 3, 2021, doi: 10.26866/jees.2021.3.r.24.

[28] R. K. Goyal and U. S. Modani, "A compact mimo microsrip patch antenna design at 28 ghz for 5g smart phones," *International Journal of Engineering Research & Technology*, vol. 9, no. 4, 2021, doi:10.17577/IJERTCONV9IS04001.

[29] M. Hussain *et al*., "Design and characterization of compact broadband antenna and its mimo configuration for 28 ghz 5g applications," *Electronics*, vol. 11, no. 4, p. 523, 2022, doi:10.3390/electronics11040523.

BIOGRAPHIES OF AUTHORS

Md. Sohel Rana postgraduate research student in electrical and electronic engineering from the Bangladesh University of Engineering and Technology (BUET), Bangladesh. Received the B.Sc. in Electrical and Electronic Engineering from the Rajshahi University of Engineering and Technology (RUET), Rajshahi, Bangladesh, in 2014. He has been with the Department of Electrical and Electronic Engineering, Daffodil International University (DIU), Bangladesh where he is currently Senior Lecturer. He has authored a number of internationally published papers. His publications focus on antenna design, wireless communication, underwater communication, 5G and 6G cellular network, mmWave Technology. He was a Telecom Engineer at Robi Axiata Limited, Bangladesh for about 2 years. He can be contacted at email: sohel.eee@diu.edu.bd.

Md. Nahid Hasan obtained a BSc Degree in Electrical and Electronic Engineering from Daffodil international university in 2023. His research interest includes microstrip patch antenna, stability analysis of power system, renewable energy, and nano technology. He can be contacted at email: nahid33-820@diu.edu.bd.

Dr. Mohammad Faisal the individual earned a Ph.D. in Electrical, Electronic and Information Engineering from Osaka University, Japan, in March 2010. Currently a Professor at the Department of Electrical and Electronic Engineering, BUET, he has authored over 70 international publications spanning fiber-optic communication systems, ultra high-speed long haul transmission, fiber nonlinearities, and photonic crystal fiber based optical waveguides, among others. A senior member of IEEE and former member of IEB, he also serves as an executive member of IEEE Communications Society Bangladesh Chapter. He can be contacted at email: mdfaisal@eee.buet.ac.bd.

Md. Emran Khan obtained a BSc degree in Electrical and Electronic Engineering from Daffodil international university in 2023. His research interest includes microstrip patch antenna, solid state, renewable energy, and nano technology. He can be contacted at email: emran33-1017@diu.edu.bd.